Realizing Small Energy Loss of 0.55 eV, High Open-Circuit Voltage >1 V and High Efficiency >10% in Fullerene-Free Polymer Solar Cells via Energy Driver

*Pei Cheng, Mingyu Zhang, Tsz-Ki Lau, Yao Wu, Boyu Jia, Jiayu Wang, Cenqi Yan, Meng Qin, Xinhui Lu, and Xiaowei Zhan**

A solar cell is developed as a renewable clean energy technology to overcome the energy and environmental problems. Especially, bulk heterojunction (BHJ) organic solar cells (OSCs) have attracted considerable attention in the past decade since they present some advantages, such as simple preparation, light weight, low cost, flexibility, and semitransparency.[1–6] Recently, BHJ OSCs based on interpenetrating networks of low-bandgap (LBG) donor polymers and fullerene acceptors (e.g., PCBM) exhibited the best performance with power conversion efficiencies (PCEs) >11%.[7–9]

In the last decade, one of the most important progresses in the research field of OSCs is developing LBG donor polymers.[10–14] LBG polymers can broaden the absorption of OSCs into near-infrared (NIR) region due to their relatively lower optical bandgaps.[15–22] As a result, OSCs based on LBG donor polymers and PCBM exhibit very high short-circuit current density (J_{SC}) (16-22 mA cm^{-2}).[7–9,23–26] However, because of the relatively higher highest occupied molecular orbital (HOMO) energy levels of LBG donor polymers, the open-circuit voltage (V_{OC}) of these OSCs is generally lower than 0.8 V, which limits the further increase in PCE. In order to increase the V_{OC} in the OSCs based on LBG polymers and PCBM, the lowest unoccupied molecular orbital (LUMO) energy levels of fullerene acceptors are upshifted by chemical modifications. As a result, the V_{OC} of the OSCs can be obviously increased due to the increased energy offset between the HOMO energy level of donor (D) and the LUMO energy level of acceptor (A). However, the upshifted LUMO energy level of acceptor will decrease the energy offset between the LUMO energy levels of donor and acceptor, which will reduce the driving force for charge transfer (ΔG_{CT}) from donor to acceptor and therefore decrease the J_{SC} and fill factor (FF). For example, indene-C_{60} bisadduct (ICBA) has relatively higher LUMO energy level than that of PCBM, the OSCs based on ICBA and poly(3-hexylthiophene) (a mid-bandgap donor with very high LUMO energy level) exhibit good performance,[27–29] due to enough ΔG_{CT} value (≈ +0.18 eV).[30] However, ICBA works poorly with LBG donor polymers that possess low LUMO energy levels, partially due to insufficient ΔG_{CT} value (≈ −0.05 eV).[30] Compared with the OSCs based on LBG polymers and PCBM, the OSCs based on LBG polymers and ICBA exhibit enhanced V_{OC} (≈ 0.9–1.0 V) but decreased J_{SC} (≈ 8–10 mA cm^{-2}) and FF (≈ 50%), leading to low PCEs of <5%.[31–34]

Compared with fullerene acceptors, nonfullerene acceptors possess broad and strong absorption in visible and NIR region and tunable energy levels, and have attracted increasing attention in recent years.[35–40] In fullerene-free OSCs, there not only exists "channel I" for charge generation (exciton generation at donor, charge transfer from donor to acceptor), but also "channel II"[41] for charge generation (exciton generation at acceptor, charge transfer from acceptor to donor). Thus, sufficient driving force for charge transfer in both channels becomes critical to the performance of fullerene-free OSCs.

Herein, we report a new, easy and efficient approach to enhance the driving force for charge transfer, to break tradeoff between V_{OC} and J_{SC}, and to simultaneously achieve very small energy loss (0.55 eV), very high V_{OC} (>1 V) and very high PCE (>10%) in fullerene-free OSCs via energy driver. PTB7-th is a famous LBG donor polymer with broad absorption,[42] while IDT-2BR is a nonfullerene small molecule acceptor with broad absorption and high LUMO energy level developed by our group (**Figure 1**b).[43] These two materials exhibit insufficient LUMO energy offset and insufficient HOMO energy offset between donor and acceptor. In order to enhance the driving force for charge transfer in the OSCs based on PTB7-th/IDT-2BR, we employed a conjugated molecule PDI-2DTT[44] (Figure 1a) as the third component[45–49] in the active layer. Compared with IDT-2BR, PDI-2DTT has lower LUMO and HOMO energy levels, which can act as an "energy driver" to enhance the driving force for charge transfer. As a result, compared with the OSCs without PDI-2DTT, the OSCs with tiny

Dr. P. Cheng
Beijing National Laboratory for Molecular Sciences
CAS Key Laboratory of Organic Solids
Institute of Chemistry
Chinese Academy of Sciences
Beijing 100190, P. R. China
Dr. P. Cheng
University of Chinese Academy of Sciences
Beijing 100049, P. R. China
M. Zhang, Y. Wu, B. Jia, J. Wang, C. Yan, Dr. M. Qin, Prof. X. Zhan
Department of Materials Science and Engineering
College of Engineering
Key Laboratory of Polymer Chemistry and Physics
of Ministry of Education
Peking University
Beijing 100871, P. R. China
E-mail: xwzhan@pku.edu.cn
T.-K. Lau, Prof. X. Lu
Department of Physics
Chinese University of Hong Kong
New Territories, Hong Kong, P. R. China

DOI: 10.1002/adma.201605216

© 2017 WILEY-VCH Verlag GmbH & Co. KGaA, Weinheim

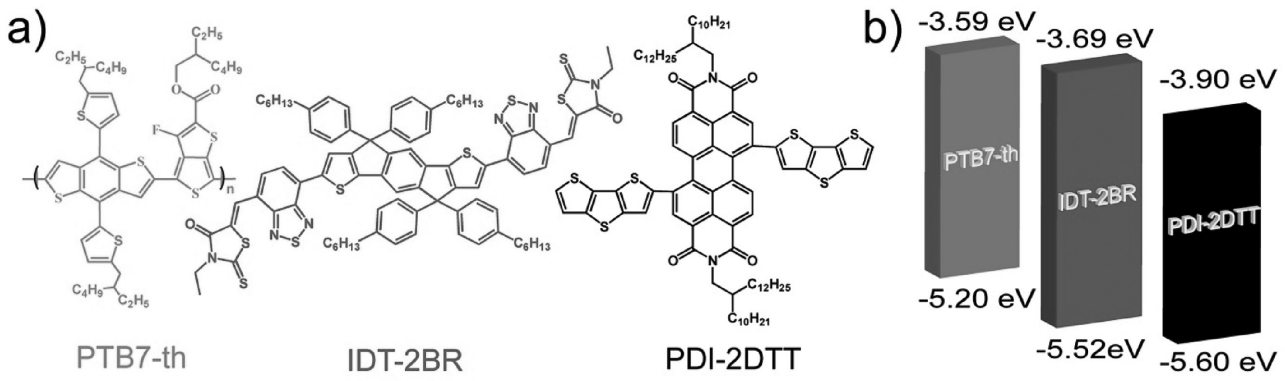

Figure 1. a) Molecule structures and b) energy levels of PTB7-th, IDT-2BR, and PDI-2DTT.

amount of PDI-2DTT (1%, the weight ratio in the active layer) exhibit enhanced average PCE from 8.2% to 9.7% with the best PCE of 10.1%, which is the highest reported for the single-junction OSCs with very small energy loss (<0.6 eV) and very high V_{OC} of >1 V.

Following the calculation method for ΔG_{CT} reported by Janssen et al.,[50] we calculate the ΔG_{CT} in PTB7-th/IDT-2BR blend and PTB7-th/PDI-2DTT blend (Table S1, Supporting Information). The ΔG_{CT} values from donor to acceptor and acceptor to donor in PTB7-th/IDT-2BR blend are –0.13 and –0.03 eV, respectively. The ΔG_{CT} values from donor to acceptor and acceptor to donor in PTB7-th/PDI-2DTT blend are +0.01 and +0.14 eV, respectively. Compared with that in PTB7-th/PDI-2DTT blend, the insufficient ΔG_{CT} in PTB7-th/IDT-2BR blend is unfavorable for efficient charge transfer.

The *J*–*V* curves and external quantum efficiency (EQE) spectra of devices based on PTB7-th/IDT-2BR or PTB7-th/IDT-2BR/PDI-2DTT under the illumination of an AM 1.5 G solar simulator (100 mW cm^{-2}) are shown in **Figure 2**. The average (calculated from 20 individual devices) and best device characteristics are summarized in **Table 1**. After addition of tiny amount PDI-2DTT (1% or 2%) to the blend of PTB7-th/IDT-2BR, the J_{SC} and FF are obviously changed but the V_{OC} still keep very high of 1.03–1.05 V. The energy loss ($E_{loss} = E_g – eV_{OC}$, where the optical bandgap E_g of blend layer is 1.58 eV) is 0.53–0.55 eV, which is the smallest value in high-performance OSCs (PCE >10%).[51–53] The J_{SC}, FF, and PCE increase first and then decrease with increasing PDI-2DTT content. Compared with the OSCs without PDI-2DTT, the OSCs with 1% PDI-2DTT exhibit enhanced performance, the average J_{SC}, FF, and PCE increase from 12.8 to 14.5 mA cm^{-2}, 61.1% to 65.0% and 8.2% to 9.7%, respectively. The best PCE of PTB7-th/IDT-2BR/1% PDI-2DTT based OSCs is 10.1%, which is the highest reported for the single junction OSCs with very high V_{OC} >1.0 V.

As shown in Figure 2b, considering the absorption spectra of PTB7-th and IDT-2BR films (Figure S1, Supporting Information), the EQE in 360–450 nm is mainly attributed to IDT-2BR; the EQE in 450–680 nm is attributed to PTB7-th and IDT-2BR; and the EQE in 680–770 nm is mainly attributed to PTB7-th. After the addition of 1% PDI-2DTT, the EQE related to both PTB7-th and IDT-2BR parts are obviously enhanced. From integration of the EQE spectra with the AM 1.5G reference spectrum, the calculated J_{SC} is obtained, which is similar to *J*–*V* measurement (the average error is 1.8%, Table 1).

The steady photoluminescence (PL) was carried out to investigate the charge transfer in OSCs. As shown in **Figure 3**a, the PL intensity of PTB7-th/IDT-2BR blend decreases by 80% and 70% relative to that of pure PTB7-th and pure IDT-2BR, respectively (the PL intensities of different films are compared at their PL peaks). The insufficient PL quenching of PTB7-th/IDT-2BR blend is related to the insufficient ΔG_{CT} from donor to acceptor and acceptor to donor. After adding 1% or 2% PDI-2DTT, the PL

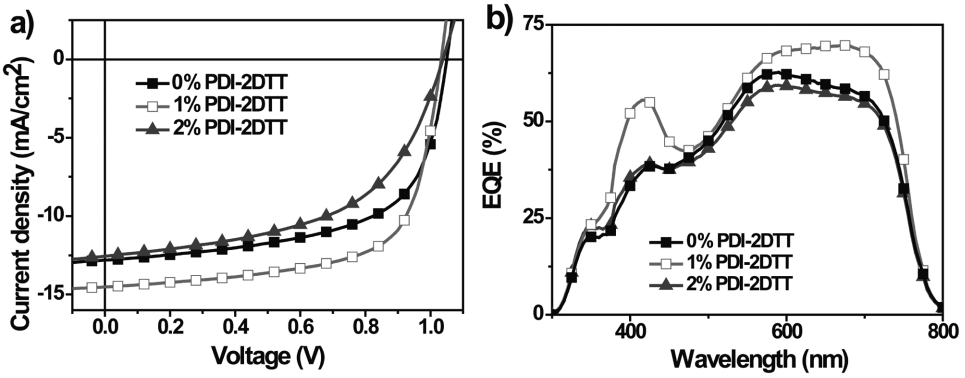

Figure 2. a) *J*–*V* curves and (b) EQE spectra of devices with the structure ITO/PEDOT:PSS/PTB7-th:IDT-2BR or PTB7-th:IDT-2BR:PDI-2DTT/Ca/Al under the illumination of an AM 1.5G solar simulator, 100 mW cm^{-2}.

© 2017 WILEY-VCH Verlag GmbH & Co. KGaA, Weinheim

Table 1. Average and best device data based on PTB7-th/IDT-2BR or PTB7-th/IDT-2BR/PDI-2DTT.

PDI-2DTT [w/w]	V_{OC} [V]	J_{SC} [mA cm^{-2}]	Calculated J_{SC} [mA cm^{-2}]	FF [%]	PCE [%]	
					Average	Best
0	1.05 ± 0.01	12.8 ± 0.2	12.6	61.1 ± 0.3	8.2 ± 0.1	8.5
1%	1.03 ± 0.01	14.5 ± 0.3	14.4	65.0 ± 0.4	9.7 ± 0.2	10.1
2%	1.04 ± 0.01	12.5 ± 0.1	12.1	52.9 ± 0.4	6.9 ± 0.1	7.1

intensity of PTB7-th/IDT-2BR blend decreases by 96% and 94% relative to that of pure PTB7-th and pure IDT-2BR, respectively. The stronger PL quenching suggests more efficient charge transfer from donor to acceptor and acceptor to donor. In order to further investigate the charge transfer in the PTB7-th/IDT-2BR blend without or with PDI-2DTT, the time resolved transient photoluminescence (TRTPL) was employed (Figure 3b). The tests were carried out by monitoring 780 nm emission under 470 nm light excitation. The calculation details of excited-state lifetimes are shown in the Supporting Information. The excited-state lifetime of PTB7-th/IDT-2BR blend film is 0.72 ns and decreased to 0.44 or 0.39 ns for PTB7-th/IDT-2BR blend film with 1% or 2% PDI-2DTT, respectively. The shorter lifetime indicates higher proportional photoinduced charges being transferred. The enhanced EQE response of PTB7-th and IDT-2BR in PTB7-th/IDT-2BR/PDI-2DTT blend also indicates more efficient charge transfer from donor to acceptor and acceptor to donor. The more efficient charge transfer in PTB7-th/IDT-2BR/PDI-2DTT is attributed to the lower LUMO and HOMO energy levels of PDI-2DTT (acting as an energy driver). The more efficient charge transfer is beneficial to enhancement in J_{SC}, FF, and PCE of OSCs.

Grazing-incidence wide-angle X-ray scattering (GIWAXS) and grazing-incidence small-angle X-ray scattering (GISAXS) measurements were carried out to figure out the effect of the energy driver (PDI-2DTT) on film morphology of PTB7-th/IDT-2BR. GIWAXS can provide molecular-level structural information such as lattice constant, crystallinity, and orientation of polymer packing,[54–56] while GISAXS can provide larger length-scale phase separation information (such as hundreds nanometers).[57] The 2D GIWAXS patterns of PTB7-th/IDT-2BR without or with PDI-2DTT are shown in **Figure 4**a. The molecular packing in PTB7-th/IDT-2BR/1% PDI-2DTT film is similar to that of PTB7-th/IDT-2BR film in terms of polymer crystallite orientation, as indicated by the similar ring-like lamellar peak at $q = 0.3$ Å^{-1}. In contrast, when the addition amount of PDI-2DTT is increased from 1% to 2%, the molecular packing behavior of the blend film becomes quite different. Two peaks were observed at $q = 0.3$ and 0.4 Å^{-1}, suggesting that both PTB7-th and IDT-2BR crystallites were formed. However, this formation seems not beneficial to the device performance. Corresponding 2D GISAXS patterns are shown in Figure 4b. Figure S2 in the Supporting Information shows the in-plane scattering intensity profiles. By fitting the profiles with models presented in previous studies,[39,58] we can roughly estimate the domain size of each phase. Consistent with GIWAXS results, the GISAXS profiles of PTB7-th/IDT-2BR and PTB7-th/IDT-2BR/1% PDI-2DTT are similar, suggesting similar degree of nanoscale phase separation. Here, since pure PTB7-th shows stronger scattering than pure IDT-2BR and pure PDI-2DTT (Figure S3, Supporting Information), it is reasonable to attribute the fitting results to PTB7-th domain sizes instead of IDT-2BR and PDI-2DTT. The fitted PTB7-th domain sizes of PTB7-th/IDT-2BR and PTB7-th/IDT-2BR/1% PDI-2DTT films are both comparable to theoretical exciton diffusion length (8.6 and 11.1 nm, respectively), capable of efficient exciton dissociation. After increasing the addition amount of PDI-2DTT from 1% to 2%, the GISAXS pattern experiences much larger changes as the fitted PTB7-th domain size increases to 30.1 nm, suggesting excessively large D/A phase separation in PTB7-th/IDT-2BR film with 2% PDI-2DTT, which accounts for the low J_{SC} and FF of the corresponding OSCs.

Space charge limited current (SCLC) method[59] was employed to measure the hole mobility and electron mobility of PTB7-th/IDT-2BR blend films without or with PDI-2DTT. Hole-only and electron-only diodes were fabricated using the architectures: indium tin oxide (ITO)/poly(3,4-ethylenedioxythiophene):poly(styrene sulfonate) (PEDOT:PSS)/active layer/gold (Au) for holes and aluminum (Al)/active layer/Al for electrons. The J–V curves of the devices are plotted as $\ln[Jd^3/(V_{appl}-V_{bi})^2]$ versus $[(V_{appl}-V_{bi})/d]^{0.5}$ (**Figure 5**). The hole mobilities and electron mobilities are calculated and listed in **Table 2**. After the addition of 1% PDI-2DTT into PTB7-th/IDT-2BR blend, the hole mobility and electron mobility of the blend film are 1.6×10^{-4} and 3.8×10^{-4} cm^2 V^{-1} s^{-1}, respectively, similar to that of

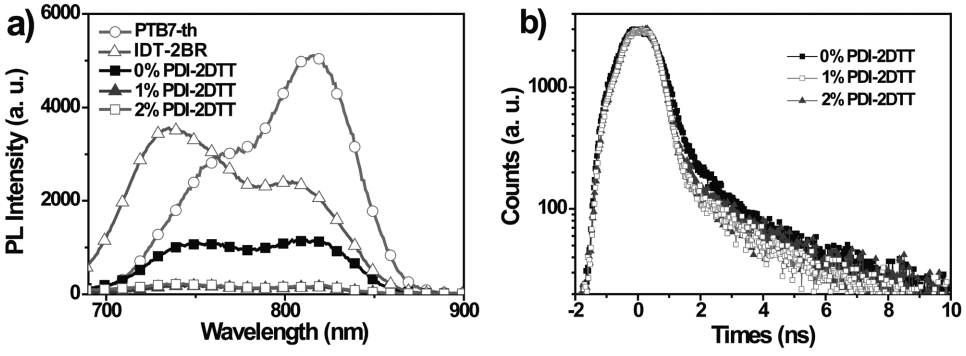

Figure 3. a) PL spectra of PTB7-th, IDT-2BR, PTB7-th/IDT-2BR, and PTB7-th/IDT-2BR/PDI-2DTT films. b) TRTPL spectra of PTB7-th/IDT-2BR and PTB7-th/IDT-2BR/PDI-2DTT films.

© 2017 WILEY-VCH Verlag GmbH & Co. KGaA, Weinheim

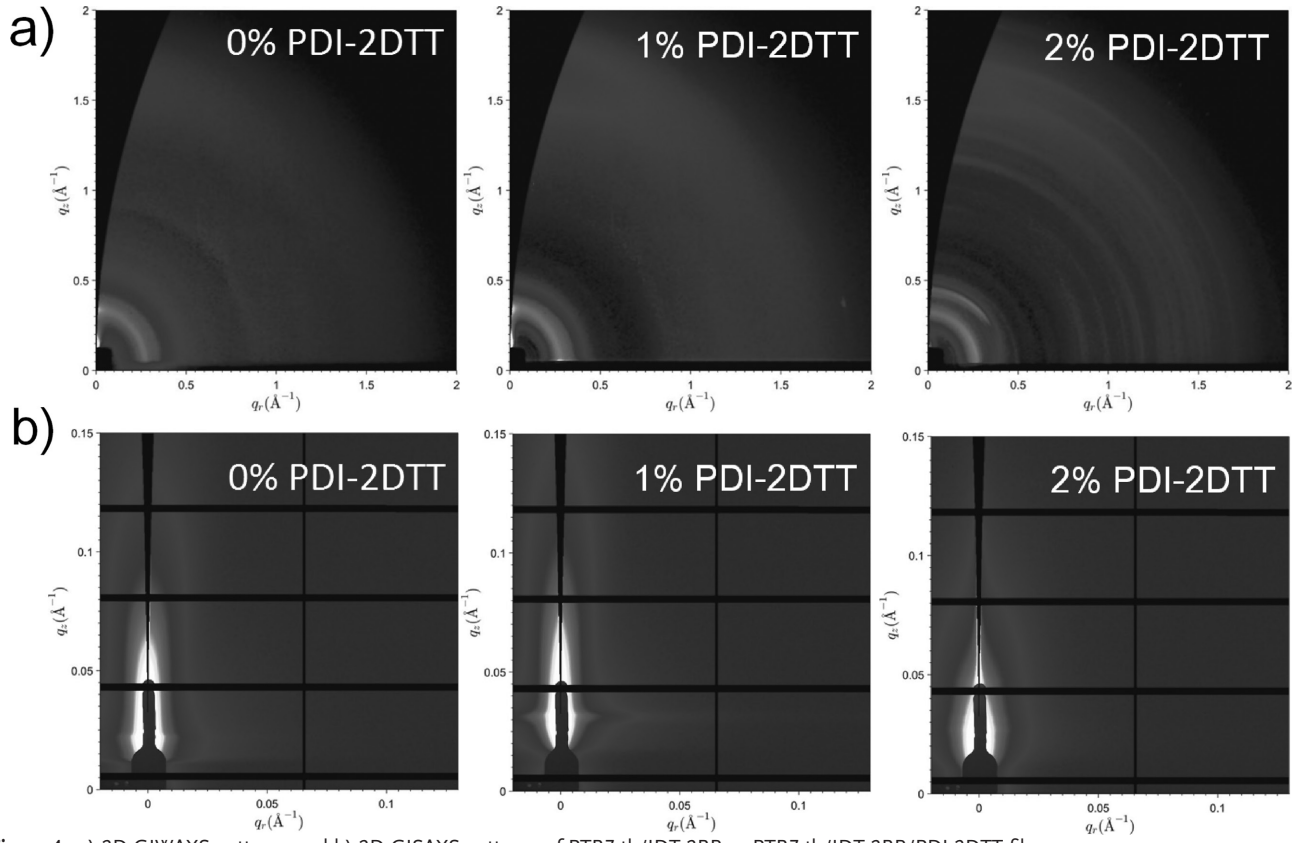

Figure 4. a) 2D GIWAXS patterns and b) 2D GISAXS patterns of PTB7-th/IDT-2BR or PTB7-th/IDT-2BR/PDI-2DTT films.

PTB7-th/IDT-2BR blend film without PDI-2DTT (1.8×10^{-4} and 4.1×10^{-4} cm^2 V^{-1} s^{-1}). While the mobility of the blend film decreases sharply after adding 2% PDI-2DTT, the hole mobility and electron mobility of this film are 6.2×10^{-5} and 1.5×10^{-4} cm^2 V^{-1} s^{-1}, respectively. Compared with PTB7-th/IDT-2BR film and PTB7-th/IDT-2BR/1%PDI-2DTT film, the lower mobility of PTB7-th/IDT-2BR/2%PDI-2DTT film is related to the changed morphology observed in GIWAXS and GISAXS (Figure 4).

To further investigate the charge generation and collection efficiencies in PTB7-th/IDT-2BR film without or with PDI-2DTT, the corrected photocurrent measurement was employed. According to the calculation method reported by Nelson et al.,[33] the corrected photocurrent is defined as the device current under illumination as a function of voltage after subtraction of the corresponding dark current ($J_{ph} = J_{light} - J_{dark}$). When the high reverse biases are applied, the J_{ph} becomes saturation (J_{sat}). **Figure 6** shows J_{ph}/J_{sat} for PTB7-th/IDT-2BR film without or with PDI-2DTT over a range of bias (V_0–V, where V_0 is the voltage at which the currents measured under illumination and in the dark are equal). The ratio of J_{ph} to J_{sat} represents the product of charge generation and collection efficiencies. In OSCs, there are three steps in charge generation and collection: charge transfer, charge transport and charge extraction. In

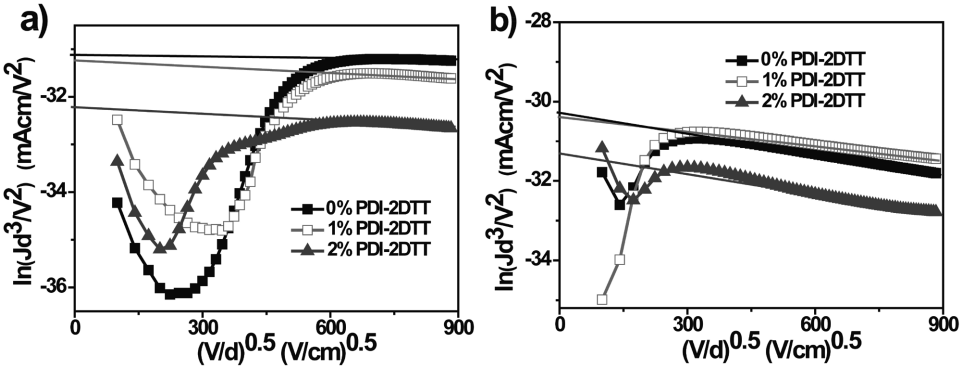

Figure 5. a) Hole-only and b) electron-only devices based on PTB7-th/IDT-2BR or PTB7-th/IDT-2BR/PDI-2DTT films.

© 2017 WILEY-VCH Verlag GmbH & Co. KGaA, Weinheim

Table 2. Hole mobilities and electron mobilities of PTB7-th/IDT-2BR or PTB7-th/IDT-2BR/PDI-2DTT films.

PDI-2DTT [w/w]	μ_h [$cm^2\ V^{-1}\ s^{-1}$]	μ_e [$cm^2\ V^{-1}\ s^{-1}$]
0	1.8×10^{-4}	4.1×10^{-4}
1%	1.6×10^{-4}	3.8×10^{-4}
2%	6.2×10^{-5}	1.5×10^{-4}

this work, the charge extraction of all three devices is similar due to the same device geometry, interlayers and electrodes. Thus, J_{ph}/J_{sat} represents the product of charge transfer and charge transport efficiencies. At low V_0–V (<10 V), i.e., at low electric field, the J_{ph}/J_{sat} of PTB7-th/IDT-2BR/1% PDI-2DTT film is higher than that of PTB7-th/IDT-2BR film and PTB7-th/IDT-2BR/2% PDI-2DTT film. Compared with PTB7-th/IDT-2BR film, the PTB7-th/IDT-2BR/1% PDI-2DTT film exhibits similar morphology and similar charge carrier mobilities, thus, the improved charge transfer is the reason for the enhanced J_{ph}/J_{sat}. The PTB7-th/IDT-2BR/2% PDI-2DTT film exhibits similar ability of charge transfer but excessively large D/A phase separation and lower charge carrier mobilities relative to PTB7-th/IDT-2BR/1% PDI-2DTT film, which is the reason for its lower J_{ph}/J_{sat}. Therefore, the PDI-2DTT addition amount of 1% is a good choice for strong driving force for charge transfer and suitable morphology, leading to the best PCE exceeding 10%.

In summary, we used PDI-2DTT with lower LUMO and HOMO energy levels as an energy driver to enhance the driving force for charge transfer, and to simultaneously achieve very small energy loss (0.55 eV), very high V_{OC} (>1 V) and very high PCE (>10%) in fullerene-free OSCs based on PTB7-th/IDT-2BR blend. Compared with PTB7-th/IDT-2BR film without PDI-2DTT, the PTB7-th/IDT-2BR film with PDI-2DTT (1% or 2%) exhibits more efficient charge transfer between donor and acceptor. Meanwhile, when the PDI-2DTT content is only 1%, the molecular packing, donor/acceptor phase separation, and charge carrier mobility of the ternary blend are similar to those of PTB7-th/IDT-2BR, which guarantees efficient charge collection. As a result, compared with the OSCs without PDI-2DTT, the OSCs with 1% PDI-2DTT exhibit enhanced J_{SC}, FF, and PCE. The best PCE of PTB7-th/IDT-2BR/1% PDI-2DTT based OSCs is 10.1%, which is the highest reported for the single junction OSCs with very small energy loss (<0.6 eV) and very high V_{OC} (>1.0 V).

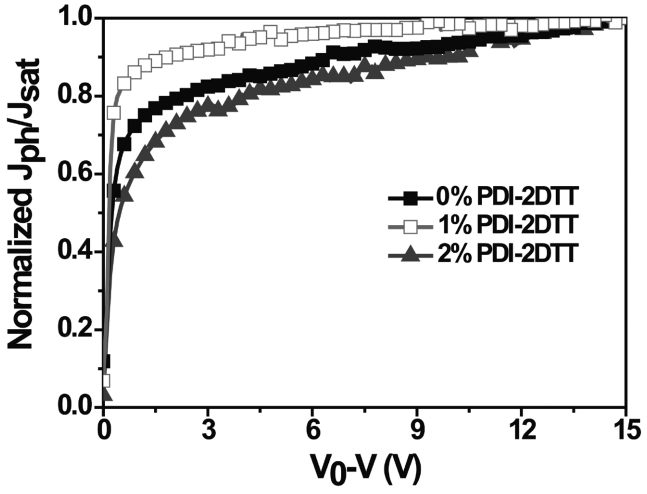

Figure 6. Corrected photocurrent data as a function of the potential difference $V_0 - V$. Data are presented for the devices based on PTB7-th/IDT-2BR or PTB7-th/IDT-2BR/PDI-2DTT films.

Supporting Information

Supporting Information is available from the Wiley Online Library or from the author.

Acknowledgements

X.Z. thanks the 973 Program (2013CB834702) and NSFC (91433114) for financial support. X.L. thanks the Research Grant Council of Hong Kong (General Research Fund No. 14303314 and Theme-based Research Scheme No. T23-407/13-N) for financial support.

Received: September 27, 2016
Revised: November 18, 2016
Published online: January 19, 2017

[1] Y.-J. Cheng, S.-H. Yang, C.-S. Hsu, *Chem. Rev.* **2009**, *109*, 5868.
[2] C. J. Brabec, M. Heeney, I. McCulloch, J. Nelson, *Chem. Soc. Rev.* **2011**, *40*, 1185.
[3] L. Lu, T. Zheng, Q. Wu, A. M. Schneider, D. Zhao, L. Yu, *Chem. Rev.* **2015**, *115*, 12666.
[4] P. Cheng, X. Zhan, *Chem. Soc. Rev.* **2016**, *45*, 2544.
[5] Y. Lin, Y. Li, X. Zhan, *Chem. Soc. Rev.* **2012**, *41*, 4245.
[6] F. C. Krebs, N. Espinosa, M. Hösel, R. R. Søndergaard, M. Jørgensen, *Adv. Mater.* **2014**, *26*, 29.
[7] J. Zhao, Y. Li, G. Yang, K. Jiang, H. Lin, H. Ade, W. Ma, H. Yan, *Nat. Energy* **2016**, *1*, 15027.
[8] L. Nian, K. Gao, F. Liu, Y. Kan, X. Jiang, L. Liu, Z. Xie, X. Peng, T. P. Russell, Y. Ma, *Adv. Mater.* **2016**, *28*, 8184.
[9] K. H. Park, Y. Ana, S. Jung, H. Park, C. Yang, *Energy Environ. Sci.* **2016**, *9*, 3464.
[10] Y. F. Li, *Acc. Chem. Res.* **2012**, *45*, 723.
[11] L. Dou, Y. Liu, Z. Hong, G. Li, Y. Yang, *Chem. Rev.* **2015**, *115*, 12633.
[12] L. Ye, S. Zhang, L. Huo, M. Zhang, J. Hou, *Acc. Chem. Res.* **2014**, *47*, 1595.
[13] C. Liu, K. Wang, X. Gong, A. J. Heeger, *Chem. Soc. Rev.* **2016**, *45*, 4825.
[14] W. Li, K. H. Hendriks, M. M. Wienk, R. A. J. Janssen, *Acc. Chem. Res.* **2016**, *49*, 78.
[15] Y. Liang, Z. Xu, J. Xia, S.-T. Tsai, Y. Wu, G. Li, C. Ray, L. Yu, *Adv. Mater.* **2010**, *22*, E135.
[16] H.-Y. Chen, J. Hou, S. Zhang, Y. Liang, G. Yang, Y. Yang, L. Yu, Y. Wu, G. Li, *Nat. Photonics* **2009**, *3*, 649.
[17] L. Dou, C.-C. Chen, K. Yoshimura, K. Ohya, W.-H. Chang, J. Gao, Y. Liu, E. Richard, Y. Yang, *Macromolecules* **2013**, *46*, 3384.
[18] Y. Liang, D. Feng, Y. Wu, S.-T. Tsai, G. Li, C. Ray, L. Yu, *J. Am. Chem. Soc.* **2009**, *131*, 7792.
[19] J. Hou, H.-Y. Chen, S. Zhang, R. I. Chen, Y. Yang, Y. Wu, G. Li, *J. Am. Chem. Soc.* **2009**, *131*, 15586.
[20] J. You, L. Dou, K. Yoshimura, T. Kato, K. Ohya, T. Moriarty, K. Emery, C.-C. Chen, J. Gao, G. Li, Y. Yang, *Nat. Commun.* **2013**, *4*, 1446.
[21] W. Li, K. H. Hendriks, A. Furlan, M. M. Wienk, R. A. J. Janssen, *J. Am. Chem. Soc.* **2015**, *137*, 2231.

© 2017 WILEY-VCH Verlag GmbH & Co. KGaA, Weinheim

[22] H. Zhou, L. Yang, A. C. Stuart, S. C. Price, S. Liu, W. You, *Angew. Chem. Int. Ed.* **2011**, *50*, 2995.
[23] Z. He, C. Zhong, S. Su, M. Xu, H. Wu, Y. Cao, *Nat. Photonics* **2012**, *6*, 591.
[24] J.-D. Chen, C. Cui, Y.-Q. Li, L. Zhou, Q.-D. Ou, C. Li, Y. Li, J.-X. Tang, *Adv. Mater.* **2015**, *27*, 1035.
[25] P. Cheng, C. Yan, T.-K. Lau, J. Mai, X. Lu, X. Zhan, *Adv. Mater.* **2016**, *28*, 5822.
[26] P. Cheng, C. Yan, Y. Wu, J. Wang, M. Qin, Q. An, J. Cao, L. Huo, F. Zhang, L. Ding, Y. Sun, W. Ma, X. Zhan, *Adv. Mater.* **2016**, *28*, 8021.
[27] Y. J. He, H. Y. Chen, J. H. Hou, Y. F. Li, *J. Am. Chem. Soc.* **2010**, *132*, 1377.
[28] G. Zhao, Y. He, Y. Li, *Adv. Mater.* **2010**, *22*, 4355.
[29] C. Y. Chang, C. E. Wu, S. Y. Chen, C. H. Cui, Y. J. Cheng, C. S. Hsu, Y. L. Wang, Y. F. Li, *Angew. Chem. Int. Ed.* **2011**, *50*, 9386.
[30] T. E. Kang, H.-H. Cho, C.-H. Cho, K.-H. Kim, H. Kang, M. Lee, S. Lee, B. Kim, C. Im, B. J. Kim, *ACS Appl. Mater. Interfaces* **2013**, *5*, 861.
[31] D. Di Nuzzo, G.-J. A. H. Wetzelaer, R. K. M. Bouwer, V. S. Gevaerts, S. C. J. Meskers, J. C. Hummelen, P. W. M. Blom, R. A. J. Janssen, *Adv. Energy Mater.* **2013**, *3*, 85.
[32] E. T. Hoke, K. Vandewal, J. A. Bartelt, W. R. Mateker, J. D. Douglas, R. Noriega, K. R. Graham, J. M. J. Fréchet, A. Salleo, M. D. McGehee, *Adv. Energy Mater.* **2013**, *3*, 220.
[33] M. A. Faist, S. Shoaee, S. Tuladhar, G. F. A. Dibb, S. Foster, W. Gong, T. Kirchartz, D. D. C. Bradley, J. R. Durrant, J. Nelson, *Adv. Energy Mater.* **2013**, *3*, 744.
[34] N. C. Miller, S. Sweetnam, E. T. Hoke, R. Gysel, C. E. Miller, J. A. Bartelt, X. Xie, M. F. Toney, M. D. McGehee, *Nano Lett.* **2012**, *12*, 1566.
[35] Y. Lin, X. Zhan, *Mater. Horiz.* **2014**, *1*, 470.
[36] C. B. Nielsen, S. Holliday, H.-Y. Chen, S. J. Cryer, I. McCulloch, *Acc. Chem. Res.* **2015**, *48*, 2803.
[37] A. Facchetti, *Mater. Today* **2013**, *16*, 123.
[38] Y. Lin, J. Wang, Z.-G. Zhang, H. Bai, Y. Li, D. Zhu, X. Zhan, *Adv. Mater.* **2015**, *27*, 1170.
[39] Y. Lin, Q. He, F. Zhao, L. Huo, J. Mai, X. Lu, C.-J. Su, T. Li, J. Wang, J. Zhu, Y. Sun, C. Wang, X. Zhan, *J. Am. Chem. Soc.* **2016**, *138*, 2973.
[40] Y. Lin, F. Zhao, Q. He, L. Huo, Y. Wu, T. C. Parker, W. Ma, Y. Sun, C. Wang, D. Zhu, A. J. Heeger, S. R. Marder, X. Zhan, *J. Am. Chem. Soc.* **2016**, *138*, 4955.
[41] D. M. Stoltzfus, J. E. Donaghey, A. Armin, P. E. Shaw, P. L. Burn, P. Meredith, *Chem. Rev.* **2016**, *116*, 12920.
[42] S.-H. Liao, H.-J. Jhuo, Y.-S. Cheng, S.-A. Chen, *Adv. Mater.* **2013**, *25*, 4766.
[43] Y. Wu, H. Bai, Z. Wang, P. Cheng, S. Zhu, Y. Wang, W. Ma, X. Zhan, *Energy Environ. Sci.* **2015**, *8*, 3215.
[44] X. W. Zhan, Z. A. Tan, E. J. Zhou, Y. F. Li, R. Misra, A. Grant, B. Domercq, X. H. Zhang, Z. S. An, X. Zhang, S. Barlow, B. Kippelen, S. R. Marder, *J. Mater. Chem.* **2009**, *19*, 5794.
[45] P. Cheng, X. Zhan, *Mater. Horiz.* **2015**, *2*, 462.
[46] T. Ameri, P. Khoram, J. Min, C. J. Brabec, *Adv. Mater.* **2013**, *25*, 4245.
[47] P. P. Khlyabich, B. Burkhart, A. E. Rudenko, B. C. Thompson, *Polymer* **2013**, *54*, 5267.
[48] L. Lu, M. A. Kelly, W. You, L. Yu, *Nat. Photonics* **2015**, *9*, 491.
[49] Y. Yang, W. Chen, L. Dou, W.-H. Chang, H.-S. Duan, B. Bob, G. Li, Y. Yang, *Nat. Photonics* **2015**, *9*, 190.
[50] D. Veldman, S. C. J. Meskers, R. A. J. Janssen, *Adv. Funct. Mater.* **2009**, *19*, 1939.
[51] K. Kawashima, Y. Tamai, H. Ohkita, I. Osaka, K. Takimiya, *Nat. Commun.* **2015**, *6*, 10085.
[52] H. Bin, Z.-G. Zhang, L. Gao, S. Chen, L. Zhong, L. Xue, C. Yang, Y. Li, *J. Am. Chem. Soc.* **2016**, *138*, 4657.
[53] J. Liu, S. Chen, D. Qian, B. Gautam, G. Yang, J. Zhao, J. Bergqvist, F. Zhang, W. Ma, H. Ade, O. Inganäs, K. Gundogdu, F. Gao, H. Yan, *Nat. Energy* **2016**, *1*, 16089.
[54] G. Li, Y. Yao, H. Yang, V. Shrotriya, G. Yang, Y. Yang, *Adv. Funct. Mater.* **2007**, *17*, 1636.
[55] X. Lu, H. Hlaing, C.-Y. Nam, K. G. Yager, C. T. Black, B. M. Ocko, *Chem. Mater.* **2015**, *27*, 60.
[56] T. Xiao, H. H. Xu, G. Grancini, J. Q. Mai, A. Petrozza, U. S. Jeng, Y. Wang, X. Xin, Y. Lu, N. S. Choon, H. Xiao, B. S. Ong, X. H. Lu, N. Zhao, *Sci. Rep.* **2014**, *4*, 5211.
[57] H.-C. Liao, C.-S. Tsao, T.-H. Lin, C.-M. Chuang, C.-Y. Chen, U. S. Jeng, C.-H. Su, Y.-F. Chen, W.-F. Su, *J. Am. Chem. Soc.* **2011**, *133*, 13064.
[58] J. Mai, T.-K. Lau, J. Li, S.-H. Peng, C.-S. Hsu, U. S. Jeng, J. Zeng, N. Zhao, X. Xiao, X. Lu, *Chem. Mater.* **2016**, *28*, 6186.
[59] G. G. Malliaras, J. R. Salem, P. J. Brock, C. Scott, *Phys. Rev. B* **1998**, *58*, 13411.

© 2017 WILEY-VCH Verlag GmbH & Co. KGaA, Weinheim